Energy Proceedings
Vol 40, 2024
ISSN 2004-2965

Investigation on frost free air source heat pump system integrated with recirculated regenerated desiccant wheel

Minqi Su[1,2], Xuan Wu[1], Yuanyuan Zhou[1], Xiaoqu Han [1*], Jiping Liu[2], Junjie Yan[1]

1 State Key Laboratory of Multiphase Flow in Power Engineering, Xi'an Jiaotong University, Xi'an 710049, China

2 MOE Key Laboratory of Thermal Fluid Science and Engineering, Xi'an Jiaotong University, Xi'an 710049, China
(*Xiaoqu Han: hanxiaoqu@mail.xjtu.edu.cn)

ABSTRACT

In regions of southern China characterized by low winter temperatures and high relative humidity, frost-related challenges are frequently encountered by air source heat pumps. Traditional defrosting methods have been found to be inefficient and to yield unstable results. Therefore, an innovative frost-free air source heat pump system integrated with a recirculated regenerated desiccant wheel was proposed in this study. The impact of environmental temperature, humidity, and return water temperature on system performance were numerically investigated. Key performance indices, including inlet air humidity, system COP (Coefficient of Performance), and compressor output, were investigated. It was found that, when compared to conventional air source heat pump (ASHP) systems, a 40.3% increase in COP was achieved by the integration of the recirculated regenerative desiccant wheel. The system compressor output was significantly influenced by the ambient humidity (φ_{amb}). When absolute humidity surpassed 4.4 g·kg^{-1}, the compressor output decreased with increasing φ_{amb}. Significantly, the system performance improvement was more pronounced in conditions of higher ambient humidity. A 10% increase in relative humidity resulted in a significant 3.7% increase in COP. In summary, this study substantiates the system's reliability across diverse operating conditions, affirming its practical viability.

Keywords: frost free, air source heat pump, desiccant wheel, recirculated regenerated

NONMENCLATURE

Abbreviations	
ASHP	Air Source Heat Pump
COP	Coefficient of performance
DW	Desiccant wheel
FFASHP	Frost Free Air Source Heat Pump
Symbols	
c_p	Specific heat
m	Mass flow rate
Q_h	Heating capacity
T	Temperature
φ	Relative humidity
ω	Humidity ratio
W_e	Compressor output

1. INTRODUCTION

Air source heat pumps, constituting a commanding 90% of the current heat pump market, stand as the predominant choice owing to their economic operation and impressive energy-saving attributes [1]. The air source heat pump presents a distinctive challenge of frosting during winter conditions, particularly in the humid environs of southern China where temperatures linger around 0°C and relative humidity peaks at 80%. The onset of frosting not only diminishes the efficiency of the heat transfer process between the heat exchanger and the ambient air but also poses a threat to the safety and stability of the entire system [2].

To prevent the occurrence of frosting, extensive research has been conducted, encompassing mechanisms of frosting [3], post-frosting performance [4], and various techniques for frost prevention and removal [5]. Current methods for preventing frost can be classified into three primary types. The most conventional among them is reverse cycle defrosting. This involves manipulating the refrigerant flow direction through a four-way reversing valve, leading to the generation of superheated vapor directed toward outdoor pipes for the defrosting process [6]. However, this method is not without its challenges, potentially

This is a paper for 15th International Conference on Applied Energy (ICAE2023), Dec. 3-7, 2023, Doha, Qatar.

introducing temperature discrepancies within rooms, energy inefficiencies, and uneven defrosting.

Electric heating defrosting offers abundant defrosting energy, maintains system heating process stability, and boasts straightforward installation, thereby enhancing overall room thermal comfort. In a study conducted by Kwak and Bai [7], electric heaters were strategically incorporated into a heat pump unit, ensuring sustained system operation over a 200-minute duration. This integration resulted in a 9.1% augmentation in heat supply at an ambient temperature of 4 °C. Another investigation by Kim et al. [8] implemented an electric heater within a heat accumulator, elevating both the refrigerant temperature at the compressor's inlet and the refrigerant flow. This intervention led to a notable 15% enhancement in system defrosting efficiency and a simultaneous 15% reduction in defrosting time at an ambient temperature of −5 °C. The substantial consumption of high-grade electric energy during electric heating and defrosting raises concerns about elevated power consumption, reduced Coefficient of Performance (COP), and increased costs, rendering it less suitable for implementation in medium- and large-scale devices [9]. Zhang et al. [10] conducted both experimental and modeling investigations into the characteristics of frost distribution along the edges of a finned tube heat exchanger. Yao et al. [11] formulated a mathematical model for a three-row outdoor coil within an Air Source Heat Pump (ASHP) unit, with subsequent simulation of the frosting parameters affecting the outdoor coil. Ye et al. [12] presented a numerical model, grounded in experimental findings, to anticipate the performance of fin-and-tube heat exchangers within an ASHP unit, incorporating considerations for airflow reduction resulting from frost accumulation.

The Desiccant Wheel (DW) represents an advanced alternative to conventional electric heating for achieving effective dehumidification. Its capacity to utilize waste heat and its environmentally friendly attributes align with the objectives of energy efficiency and sustainability [13]. The DW comprises two integral sections: a dehumidification section and a regeneration section [14]. Moisture is extracted from the process air in the dehumidification section through the adsorption process facilitated by the vapor pressure difference between the desiccants and the air. Subsequently, the desiccants undergo desorption in the regeneration section [15]. This process enhances the system's dehumidification capacity by eliminating moisture from unsaturated humid air. Su et al. [16] proposed a recirculated regenerative DW dehumidification system. Improved dehumidification efficiency and exergy efficiency could be achieved by the proposed system [17]. Therefore, integration of DW with air source heat pump has emerged as a highly compelling solution.

According to the previous research, it becomes evident that numerous studies have been conducted on frost prevention technologies for heat pumps. However, the traditional methods were characterized by high energy consumption and an inability to sustain defrosting effects over an extended period. In response to these challenges, a novel frost-free air source heat pump is proposed in this paper. This system integrates a rotor to dehumidify the incoming air of the air source heat pump, providing an effective and enduring solution to the frost-related challenges faced by air source heat pumps. A comprehensive theoretical model is established for the newly proposed air source heat pump system in this study. The impact of varying ambient temperatures, ambient humidity levels, and the return water temperature of the heat network on the system's performance is explored. This investigation serves as a critical theoretical foundation for the practical implementation of the proposed system.

2. SYSTEM DESCRIPTION

2.1 Frost free air source heat pump

The frost-free air source heat pump system(FFASHP) proposed in the manuscript, depicted in Fig. 1, operates within three distinct cycles: the air cycle, refrigerant cycle, and the return water cycle. The air circulation initiates as ambient cold air is drawn into the desiccant wheel (point 1) for dehumidification via the fan. Then, the cold and dry air (point 2) acts as the cold source for the condenser (point 3). After that, the air is heating to the desired temperature in the heater for serving as the regeneration air of the DW (point 4). Finally, the hot and humid air was exhausted to the outside (point 5). The refrigerant cycle, operating as a compression heat pump cycle, begins with the compression of the refrigerant by the compressor (point 6). Then, the refrigerant serves as the heat source for heating the water in the heat exchanger (point 7). After that, the refrigerant passes through the expansion valve (point 8), and entering the evaporator to form the circulation (point 9). The water was heated in the condenser (point 10) and then was delivered to the user side. Part of the hot was served as the heat source for the regeneration air (point 11).

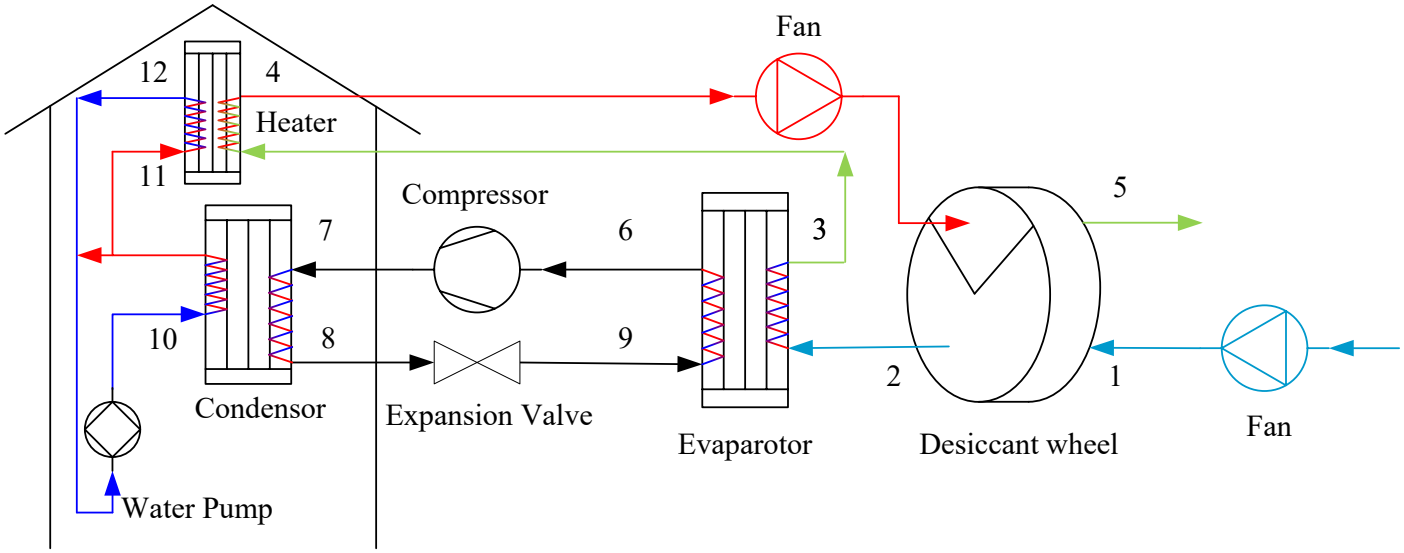

Fig. 1. Working Principle of the FFASHP integrated with recirculated regenerative desiccant wheel

2.2 Performance indices

The Coefficient of Performance (COP) of the system stands as a pivotal metric for assessing the efficacy of a heat pump. Its formulation is articulated as follows:

$$\mathrm{COP} = \frac{Q_h}{W_{\mathrm{tot}}} \qquad (1)$$

where Q_h is the heating capacity of the system, kJ·s^{1}: W_{tot} is the total work of the system, kJ·s. Q_h can be calculated as follows:

$$Q_h = c_p m\left(t_9 - t_8\right) \qquad (2)$$

where c_p is the specific heat capacity of the refrigerant, kJ·(kg·K)$^{-1}$; m is the mass flow rate of the refrigerant, kg·s^{-1};

W_{tot} can be derived as follows:

$$W_{\mathrm{tot}} = W_e + W_{\mathrm{fan}} + W_{\mathrm{DW}} \qquad (3)$$

where W_e is the output of the compressor, kJ·s^{-1}; W_{fan} is the energy consumption of the fans, kJ·s^{-1}; W_{DW} is the energy consumption the desiccant wheel, kJ·s^{-1}.

2.3 Desiccant wheel model

In the present work, a mathematical model based on the one-dimensional GSR model was established for the FFASHP system [18]. The model was established based on the following assumptions.

(1) Air resistance on the solid side was not considered.

(2) The thermodynamic characteristics of the desiccant, vapor, and air stayed consistent.

(3) The heat and mass transfer coefficient between the desiccant wall and air remained uniform along the air channel.

(4) No air leaked.

(5) The rates of material and air flow at the desiccant wheel inlet were maintained at a constant level.

The governing equations of the desiccant wheel model was as follows:

The mass conservation equation between the air and desiccant is derived as:

$$\frac{\partial \omega_a}{\partial \tau} + V\frac{\partial \omega_a}{\partial z} + \frac{f_d}{2A\rho_a}\frac{\partial \omega_d}{\partial \tau} = 0 \qquad (4)$$

The mass conservation in the desiccant can be calculated as:

$$\frac{\partial W}{\partial \tau} + \frac{2K_y P}{f_d}(\omega_d - \omega_a) = 0 \qquad (5)$$

The energy conservation between air and desiccant takes the form:

$$\frac{\partial T_a}{\partial \tau} + V\frac{\partial T_a}{\partial z} + \frac{f_d(c_{pd} + Wc_{pl}) + f_m c_{pm}}{2A\rho_a(c_{pa} + \omega_a c_{pv})}\frac{\partial T_w}{\partial \tau} + \frac{K_y P Q_{\mathrm{st}}}{A\rho_a(c_{pa} + \omega_a c_{pv})}(\omega_d - \omega_a) = 0 \qquad (6)$$

The heat transfer in the desiccant is expressed as follows:

$$\frac{\partial T_w}{\partial \tau}+\frac{2\alpha P}{f_d(c_{pd}+Wc_{pl})+f_m c_{pm}}(T_w-T_a)+\frac{2K_y PQ_{st}}{f_d(c_{pd}+Wc_{pl})+f_m c_{pm}}(\omega_d-\omega_a)+\frac{2K_y Pc_{pv}}{f_d(c_{pd}+Wc_{pl})+f_m c_{pm}}(\omega_d-\omega_a)(T_w-T_a)=0 \quad (7)$$

3. RESULTS AND DISCUSSION

3.1 Validation of the model

The accuracy of the DW model was confirmed through a comparison between simulated and experimental outcomes extracted from the literature [19]. Model validation was based on the air humidity at the DW outlet. The temporal variation of air humidity at the DW outlet is illustrated in Figure 4. The model demonstrated favorable agreement, with a maximum deviation of around 8.3% between the experimental and simulated values.

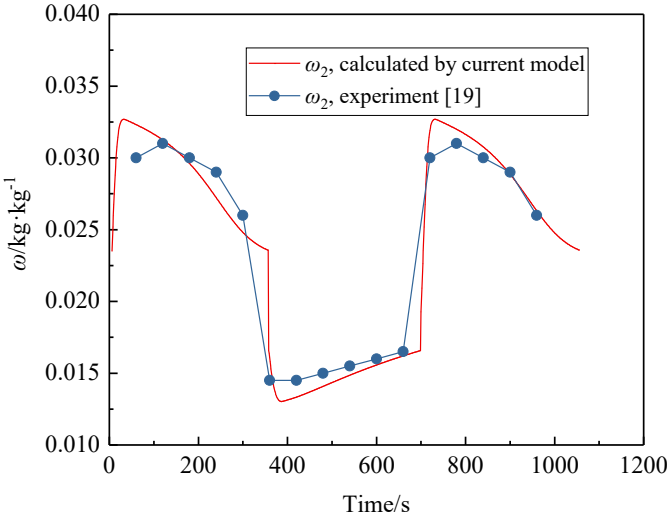

Fig. 2. Variations in specific humidity at desiccant wheel outlet with time

3.2 Influence of ambient temperature

The heat pump system is significantly influenced by the ambient temperature, especially with the rising risk of frost as temperatures decrease. Fig. 2 and Fig. 3 illustrate how the Coefficient of Performance (COP) and compressor output (W_e) varied with ambient temperature. As ambient temperature increased, there is a noticeable increase in the COP of the Frost-Free Air Source Heat Pump (FFASHP). This correlation is attributed to the higher input temperature of the air-source heat pump in warmer conditions, leading to an enhanced evaporation temperature and, consequently, improving COP.

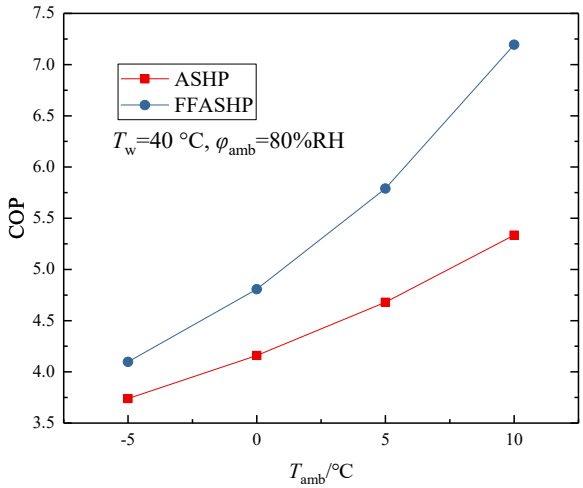

Fig. 3. Influence of T_{amb} on system COP

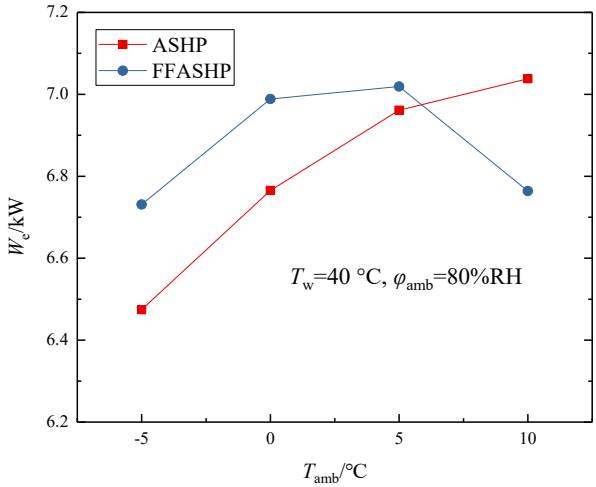

Fig. 4. Influence of T_{amb} on system W_e

It is noted that there is the substantial advancement in COP exhibited by the FFASHP in comparison to the conventional Air Source Heat Pump (ASHP), with this enhancement becoming more pronounced with increasing ambient temperature. Specifically, at 10 °C, a remarkable 40.3% superiority in COP over the ASHP was demonstrated by the FFASHP. This enhancement was ascribed to the DW dehumidification process, wherein the inlet air undergoes a temperature elevation, effectively boosting the evaporation temperature and, consequently, enhancing the COP. Therefore, the integration of DW not only signifies a marked augmentation in system efficiency but also provides a pragmatic resolution to defrosting challenges.

3.3 Influence of ambient humidity

The ambient humidity stands as a critical determinant impacting the performance of the air source heat pump. Figure 5 illustrates the intricate relationship between ambient humidity and the system's Coefficient

of Performance (COP) at 0°C. Notably, at lower temperatures, the FFASHP's COP demonstrates a linear correlation with humidity, exhibiting a 1.8% COP increase for every 10% rise in relative humidity. The possible explanation was that the input air temperature of FFASHP increased by the dehumidification of DW, resulting in an enhancement of the system's COP.

Transitioning to a higher ambient temperature of 10 °C reveals a more pronounced COP escalation with relative humidity, with a substantial 3.7% increase for every 10% RH elevation. This heightened sensitivity to ambient humidity at elevated temperatures can be attributed to the increased specific humidity in the environment. The dehumidification process of the rotor induces a more conspicuous temperature rise, magnifying the COP increment.

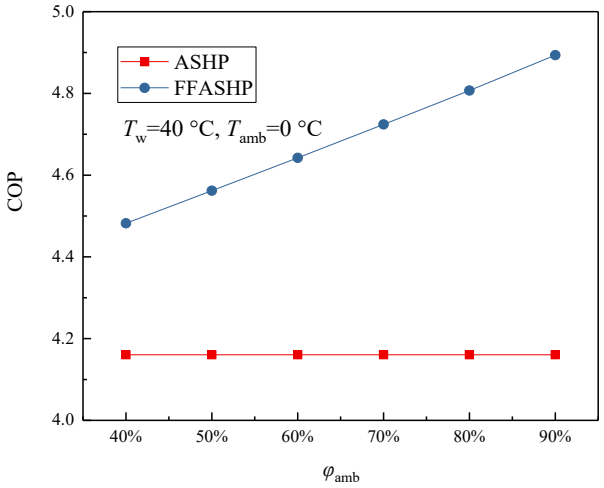

Fig. 5. Influence of φ_{amb} on system COP (T_{amb}=0 °C)

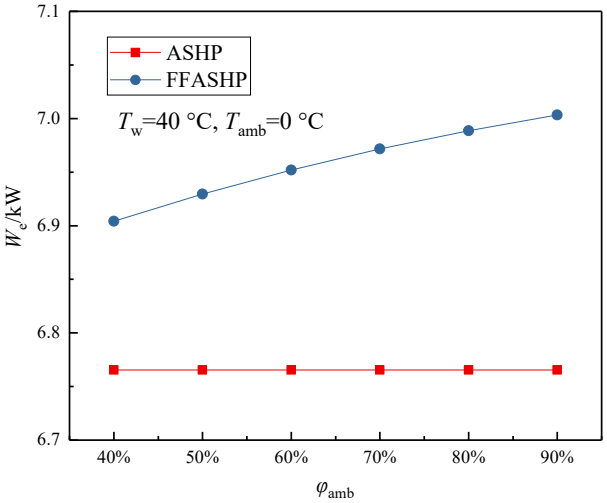

Fig. 6. Influence of φ_{amb} on system W_e (T_{amb}=0 °C)

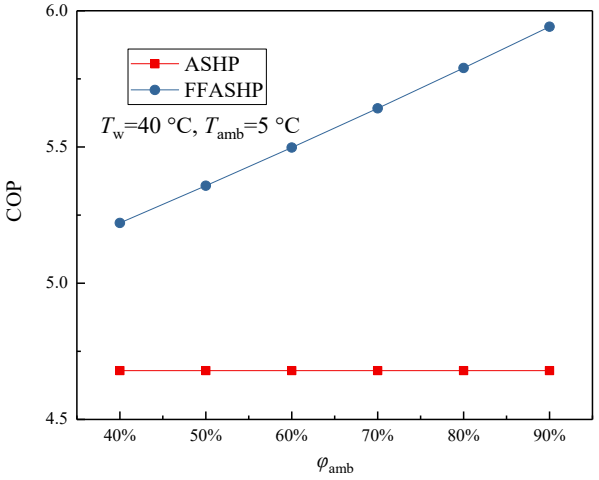

Fig. 7. Influence of T_{amb} on system COP (T_{amb}=5 °C)

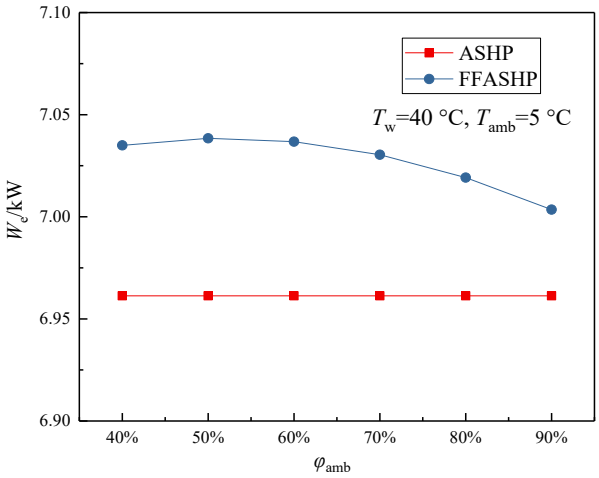

Fig. 8. Influence of T_{amb} on system COP (T_{amb}=5 °C)

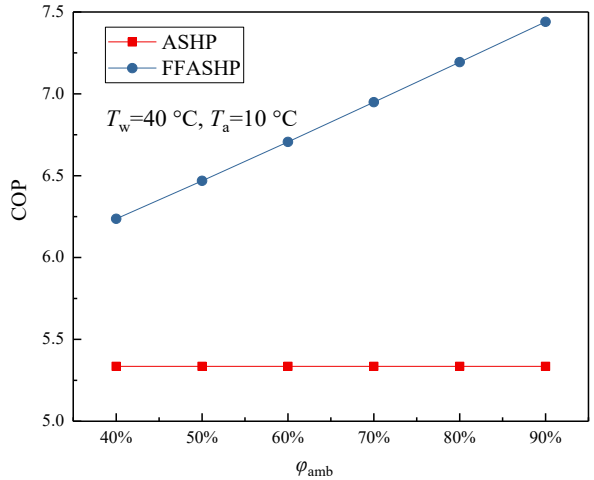

Fig. 9. Influence of T_{amb} on system COP (T_{amb}=10 °C)

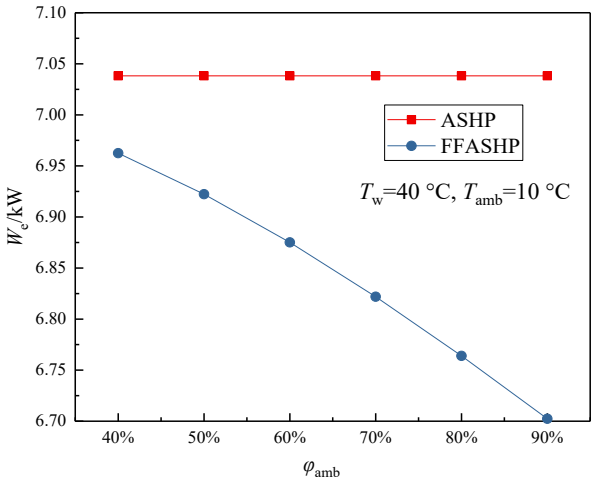

Fig. 10. Influence of T_{amb} on system W_e (T_{amb}=10 °C)

In contrast, in traditional Air Source Heat Pumps (ASHP), the energy consumption of the system remains unaffected by the humidity of the incoming air. However, a crucial consideration emerges—higher humidity heightens the risk of system frosting, escalating energy consumption during defrosting and diminishing the COP.

The impact of ambient humidity on the system's compressor output is illustrated in Fig. 6, Fig. 8 and Fig. 10. It can be observed that, at an ambient temperature of 0 °C, the compressor force increases with the rising ambient humidity. This phenomenon is attributed to the refrigerant flow rate, which, under the conditions of 0 °C ambient temperature, exceeds the rate of reduction in unit compressor power. Conversely, at an ambient temperature of 5 °C, the compressor force shows a pattern of initial increase followed by a subsequent decrease with the increase in ambient humidity. As the ambient temperature increases to 10 °C, the compressor power exhibits a declining trend in response to the increase in ambient humidity. This is due to the higher ambient temperature causing a more pronounced increase in FFASHP compressor intake temperature, leading to a more rapid reduction in unit compressor power. Importantly, it is noteworthy that the compressor output of a conventional ASHP is minimally influenced by ambient humidity.

3.4 Influence of hot water supply temperature

The supplied hot water temperature (T_w) is contingent on user demand. The impact of the supplied hot water temperature on the system COP is depicted in Fig. 11. As T_w increased, both the FFASHP and conventional ASHP exhibit a declining trend in COP. This decline is attributed to the heightened energy consumption associated with higher T_w, resulting in a COP decrease. For every 1 ℃ increase in the supply hot water temperature, the COP of FFASHP decreases by 1.1%. Notably, FFASHP maintains a higher COP compared to ASHP across various hot water supply temperatures, with the COP increasing more significantly at lower hot water supply temperatures.

The influence of T_w on W_e is illustrated in Fig. 12. It is evident that an increase in hot water supply temperature leads to an elevation in the compressor output for both systems. This rise is attributable to the increased unit compressor output with higher T_w.

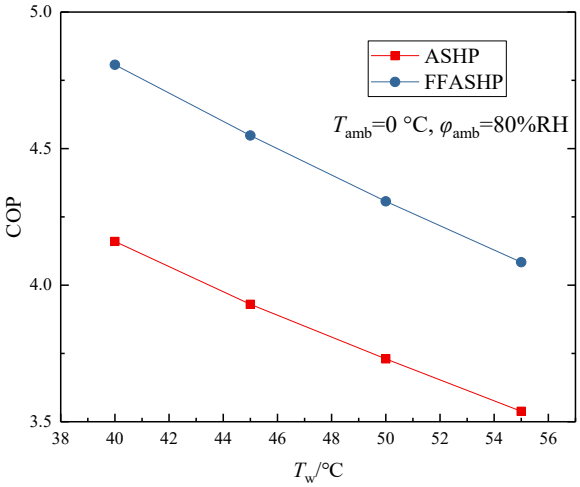

Fig. 11. Influence of T_w on system W_e (T_{amb}=10 °C)

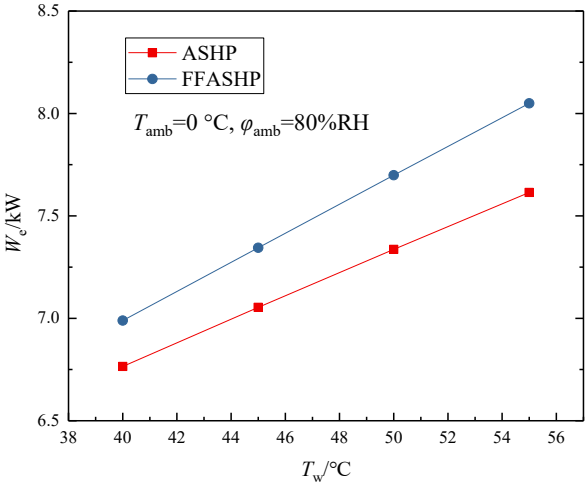

Fig. 12. Influence of T_w on system W_e (T_{amb}=10 °C)

4. CONCLUSION

A novel frost-free air source heat pump integrated with recirculated regenerative desiccant wheel was established in the present work. The influence of different parameters on its performance was theoretically investigated and the following conclusions can be drawn:

The proposed FFASHP exhibits a remarkable enhancement in performance compared to the traditional ASHP. When T_{amb} was 10 °C and φ_{amb} was 80%RH, the COP revealed a notable increase of 40.3%.

The system performance improvement was more pronounced with higher absolute humidity levels. A 10% increase in relative humidity results in a significant 3.7% increase in COP.

The system compressor output was significantly influenced by the ambient humidity. When absolute humidity surpassed 4.4 $g \cdot kg^{-1}$, the compressor output decreased with increasing φ_{amb}. Otherwise, an increase in φ_{amb} led to an elevation in compressor output.

ACKNOWLEDGEMENT

This work was supported by the National Key Research and Development Program (2022YFB4100800) and Natural Science Basic Research Plan in Shaanxi Province of China (No. 2023-JC-YB-444).

REFERENCE

[1] Yang L W, Xu R J, Hua N, et al. Review of the advances in solar-assisted air source heat pumps for the domestic sector. Energy Convers Manage 2021;247: 114710.

[2] Zhang L, Jiang Y, Dong J, et al. Advances in vapor compression air source heat pump system in cold regions: A review. Renew Sustain Energy Rev 2018;81: 353-65.

[3] Song M, Wang K, Liu S, et al. Techno-economic analysis on frosting and defrosting operations of an air source heat pump unit applied in a typical cold city. Energy Build 2018;162:65-76.

[4] Dong J, Zhang L, Deng S, et al. An experimental study on a novel radiant-convective heating system based on air source heat pump. Energy Build 2018;158:812-21.

[5] Wei W, Wu C, Ni L, et al. Performance optimization of space heating using variable water flow air source heat pumps as heating source: Adopting new control methods for water pumps. Energy Build 2022;255:111654.

[6] Qu M L, Zhang L, Chen J B, et al. Experimental analysis of heat coupling during TES based reverse cycle defrosting method for cascade air source heat pumps. Renew Energy 2020;147:35-42.

[7] Kwak K, Bai C. A study on the performance enhancement of heat pump using electric heater under the frosting condition: Heat pump under frosting condition. Appl Therm Eng 2010;30(6-7): 539-43.

[8] Kim J, Choi H J, Kim K C. A combined dual hot-gas bypass defrosting method with accumulator heater for an air-to-air heat pump in cold region. Appl Energy 2015;147:344-52.

[9] Song M, Deng S, Dang C, et al. Review on improvement for air source heat pump units during frosting and defrosting[J]. Appl Energy, 2018,211:1150-70.

[10] Zhang L, Jiang Y, Dong J, et al. An experimental study of frost distribution and growth on finned tube heat exchangers used in air source heat pump units[J]. Appl Therm Eng 2018;132:38-51.

[11] Yao Y, Jiang Y, Deng S, et al. A study on the performance of the airside heat exchanger under frosting in an air source heat pump water heater/chiller unit[J]. Int J Heat Mass Trans 2004;47(17-18):3745-56.

[12] Ye H Y, Lee K S. Performance prediction of a fin-and-tube heat exchanger considering air-flow reduction due to the frost accumulation. Int J Heat Mass Trans 2013;67:225-33.

[13] Tian S, Su X, Ge Y. Review on heat pump coupled desiccant wheel dehumidification and air conditioning systems in buildings. J Build Eng 2022;54:104655.

[14] Feng Y, Dai Y J, Wang R Z, et. al. Insights into desiccant-based internally-cooled dehumidification using porous sorbents: From a modeling viewpoint. Appl Energy 2022; 311:188732.

[15] Wu X, Ge T S, Dai Y J, et al. Review on substrate of solid desiccant dehumidification system. Renew Sustain Energy Rev 2018;82:3236-49.

[16] Su M Q, Han X Q, Chong D T, et al. Experimental study on the performance of an improved dehumidification system integrated with precooling and recirculated regenerative rotary desiccant wheel. Appl Therm Eng 2021;199:117608.

[17] Su M Q, Han X Q, Chang H Z, et al. Performance investigation and exergy analysis of a novel recirculated regenerative solid desiccant dehumidification system. J Build Eng 2023;67:106029.

[18] Na S, Chung Y, Kim MS. Performance analysis of an electric vehicle heat pump system with a desiccant dehumidifier. Energy Convers Manage 2021;236:114083.

[19] Zhang L Z, Fu H Z, Yang Q R, et al. Performance comparisons of honeycomb-type adsorbent beds (wheels) for air dehumidification with various desiccant wall materials. Energy 2014;65:430-40.